Molecular Cell
Article

eRNAs Are Required for p53-Dependent Enhancer Activity and Gene Transcription

Carlos A. Melo,[1,2,8] Jarno Drost,[1,8] Patrick J. Wijchers,[3] Harmen van de Werken,[3] Elzo de Wit,[3] Joachim A.F. Oude Vrielink,[1] Ran Elkon,[1] Sónia A. Melo,[4] Nicolas Léveillé,[1] Raghu Kalluri,[5,6] Wouter de Laat,[3] and Reuven Agami[1,7,*]

[1]Division of Gene Regulation, the Netherlands Cancer Institute, Plesmanlaan 121, 1066 CX, Amsterdam, the Netherlands
[2]Doctoral Programme in Biomedicine and Experimental Biology, Centre for Neuroscience and Cell Biology, 3004-517 Coimbra, Portugal
[3]Hubrecht Institute-KNAW and University Medical Centre Utrecht, Uppsalalaan 8, 3584CT Utrecht, the Netherlands
[4]Division of Matrix Biology, Department of Medicine, Beth Israel Deaconess Medical Center and Harvard Medical School, Boston, MA 02215, USA
[5]Department of Biological Chemistry and Molecular Pharmacology, Harvard Medical School, Boston, MA 02215, USA
[6]Harvard-MIT Division of Health Sciences and Technology, Boston, MA 02215, USA
[7]Centre for Biomedical Genetics, 3584 CG, Utrecht, the Netherlands
[8]These authors contributed equally to this work
*Correspondence: r.agami@nki.nl
http://dx.doi.org/10.1016/j.molcel.2012.11.021

SUMMARY

Binding within or nearby target genes involved in cell proliferation and survival enables the *p53* tumor suppressor gene to regulate their transcription and cell-cycle progression. Using genome-wide chromatin-binding profiles, we describe binding of p53 also to regions located distantly from any known *p53* target gene. Interestingly, many of these regions possess conserved p53-binding sites and all known hallmarks of enhancer regions. We demonstrate that these p53-bound enhancer regions (p53BERs) indeed contain enhancer activity and interact intrachromosomally with multiple neighboring genes to convey long-distance p53-dependent transcription regulation. Furthermore, p53BERs produce, in a p53-dependent manner, enhancer RNAs (eRNAs) that are required for efficient transcriptional enhancement of interacting target genes and induction of a p53-dependent cell-cycle arrest. Thus, our results ascribe transcription enhancement activity to p53 with the capacity to regulate multiple genes from a single genomic binding site. Moreover, eRNA production from p53BERs is required for efficient p53 transcription enhancement.

INTRODUCTION

The *p53* gene is the most frequently mutated gene in human cancer as mutations appear in more than 50% of tumors. In cases where tumors harbor the wild-type *p53* gene, it is believed that alterations in other p53 pathway components account for its inactivation (Vousden and Lu, 2002). Thus, the p53 tumor suppressor pathway plays a central role in tumor suppression (Christophorou et al., 2006). The *p53* gene encodes a transcription factor that regulates transcription of target genes through sequence specific interaction with DNA. As most of the inactivating mutations found in cancer are centered in its sequence-specific DNA-binding domain, regulating transcription is thought to be its main function in tumor suppression.

As a transcription factor, p53 can regulate transcription of many target genes. Its activation by different types of cellular stresses can elicit several distinct types of cellular responses, including cell-cycle arrest and apoptosis. However, the recent observation that the thus-far known protein-coding p53 target genes cannot fully explain the tumor suppression activity of p53 (Brady et al., 2011) raises the possibility that noncoding genomic regions play an important role in the p53 pathway as well. Besides the regulation of protein-coding genes, p53 has already been shown to transcriptionally regulate several noncoding RNA (ncRNA) species. These include microRNAs (miRNAs), and, more recently, p53-regulated long intergenic noncoding RNAs (lincRNAs) were also identified (Guttman et al., 2009; Huarte et al., 2010). One of these lincRNAs, termed lincRNA-p21, is specifically required for p53-dependent repression of target genes and induction of apoptosis (Huarte et al., 2010). The observation that many of the mammalian ncRNAs are highly conserved and expressed in a regulated and tissue-specific manner reflects their importance.

Chromatin-binding profiles reveal specific interactions of p53 with promoter regions of nearby target genes, but also with distant locations that harbor characteristics of enhancer domains. Enhancers are non-protein-coding domains that regulate transcription of genes at long distances and are characterized by specific chromatin signatures of histone methylation and acetylation (Birney et al., 2007; Heintzman et al., 2007, 2009). Recently, RNA polymerase II (RNAPII) was shown to bind to a subset of enhancers and produce bidirectional, nonpolyadenylated transcripts defined as enhancer RNAs (eRNAs) (Kim et al., 2010; Wang et al., 2011; De Santa et al., 2010). The transcription of these eRNAs positively correlated with the messenger RNA (mRNA) levels of the surrounding protein-coding genes (Kim et al., 2010). However, it remains unclear whether eRNAs have any function in gene transcription.

Here we identified several regions that are bound by p53 and harbor all known chromatin features of eRNA-producing enhancer domains. We named these regions p53-bound enhancer regions (p53BERs). We demonstrate that the enhancer activity of p53BERs is dependent on functional p53 and that they interact with multiple surrounding genes. The vast majority of these genes indeed display p53-dependent expression, whereas no significant p53 binding could be detected in their promoters. Furthermore, eRNAs are produced from p53BERs in a p53-dependent manner. We show that eRNAs are functional ncRNAs involved in transcription enhancement of genes interacting with the enhancer they are produced from. Thus, our results imply that p53 can regulate transcription of multiple distantly located genes through binding to enhancers and that eRNAs produced from these enhancers are involved in transcription enhancement.

RESULTS

p53 Binds to Regions Characterized by Chromatin Signatures of Enhancer Domains

The recent observation that the currently known p53 target genes do not fully account for p53-dependent tumor suppression (Brady et al., 2011) initiated our search for novel types of p53 target genes. Specifically, we searched for putative enhancer regions that are bound by p53 and thus may require p53 for their activity on target gene promoters. To identify such domains, we made use of genome-wide p53-binding data sets that we and others have generated (Wei et al., 2006; Drost et al., 2010) and ranked p53-bound regions based on p53 binding intensity (indicated by its peak height; Table S1 available online). In addition, we searched for regions that harbor histone modifications that have been shown to mark active enhancers (ENCODE Project Consortium, 2011). These include high levels of histone 3 lysine 4 monomethylation (H3K4me1), low levels of H3K4 trimethylation (H3K4me3), and high levels of H3K27 acetylation (H3K27Ac) (Heintzman et al., 2007, 2009; Creyghton et al., 2010). Several regions contained evident markers of enhancer activity combined with p53-binding at levels equivalent or higher when compared to the p21 (CDKN1A) promoter, a prominent high-affinity p53 target gene (Figures 1A, S1A, and S1B and Table S1). We named our identified enhancers *p53-b*ound *e*nhancer *r*egions (p53BERs). To confirm histone modifications also in our cell model system, we performed chromatin immunoprecipitations (ChIPs) for H3K4me1, H3K4me3, and H3K27Ac on one of our identified enhancers, p53BER2, in primary BJ fibroblasts immortalized by hTERT, the human telomerase reverse transcriptase (BJ/ET). Indeed, H3K4me1 was the predominant modification on p53BER2 in combination with high levels of H3K27Ac (marking active genomic regions [Creyghton et al., 2010]), whereas the promoter of the *p53* target gene *MDM2* harbored, as expected, predominantly H3K4me3 in combination with high levels of H3K27Ac (Figures 1B and 1C). These results confirm the enhancer signature of our identified p53BERs.

p53BERs Contain p53-Dependent Enhancer Activity

Next, we examined the potential transcriptional enhancing activity of the p53BERs using luciferase reporter assays in MCF7 cells (containing wild-type p53). We cloned 1.8–2 kb regions, including the p53BER and additional flanking sequences, upstream of a promoter driving luciferase expression. Transfection of all reporters revealed significant transcriptional enhancing activity, ranging from about 4-fold to about 190-fold, whereas two control genomic regions (harboring no enhancer features) did not show any activity in this assay (Figures 1D and S1C). Figure 1D also shows that, as expected from an enhancer region, transcription activation was orientation independent (p53BER2 reverse orientation). Importantly, the enhancer activity of all p53BERs studied here was p53 dependent, as cotransfection of a p53 knockdown vector ($p53^{KD}$) significantly inhibited enhancer activity (Figures 1D and S1C). To further confirm p53-dependency of the enhancer activity of p53BERs, we introduced point mutations in the p53 consensus sequences within p53BER2 (Figure S1B). Transfection of this reporter revealed that mutation of the p53 consensus sequence completely abolished enhancer activity of p53BER2 (Figure 1D). Altogether, we identified p53-bound regions that harbor features of enhancer domains and contain p53-dependent enhancer activity.

p53BERs Intrachromosomally Interact with Multiple Distant Genes to Convey p53-Dependent Transcription

Enhancers control expression of one or multiple genes over distance and in an orientation independent manner. This happens through so-called DNA looping, which brings the enhancer in close proximity of its target promoters (Splinter et al., 2011). Thus, p53 could potentially regulate transcription of multiple target genes through binding to a single enhancer. To identify possible target genes of p53-dependent enhancer domains, we applied chromosome conformation capture (4C) technology in combination with next-generation sequencing (Dekker et al., 2002; Splinter et al., 2011) for three p53BERs (p53BER1, p53BER2, and p53BER4) in BJ/ET cells. We found that all three p53BERs appeared to interact with multiple neighboring genes on the same chromosome (Figures 2A–2C). Similar results were obtained with two different restriction enzyme combinations (Figure S2A). Strikingly, mRNA sequencing of BJ/ET cells stably expressing either a control or p53 knockdown vector revealed that many of these genes require p53 for their proper expression (Figures 2A–2C and S2B). To confirm that these genes are indeed regulated by p53, we treated cells with the MDM2-inhibitor Nutlin-3 and analyzed mRNA levels of one prominent neighboring gene for each p53BER. These were DUSP4 (dual specificity phosphatase 4; at ~430 kb), PAPPA (pregnancy-associated plasma protein A; at ~210 kb), and IER5 (immediate early response 5; at ~50 kb), for p53BER1, p53BER2, and p53BER4, respectively. As expected, mRNA levels of all genes were induced upon Nutlin-3 treatment (Figure 2D). Moreover, knockdown of p53 decreased basal mRNA levels and interfered with the induction upon Nutlin-3 treatment (Figure 2D). These results imply that DUSP4, PAPPA, and IER5 are transcriptionally regulated by p53, though no significant p53-binding peak could be detected in their promoters by ChIP-seq in BJ/ET cells (Drost et al., 2010). Importantly, we found that the long-range interactions were still present in cells with stable p53 knockdown (Figures 2A–2C), suggesting that p53 acts on pre-existing chromatin loops to activate p53BER-target genes.

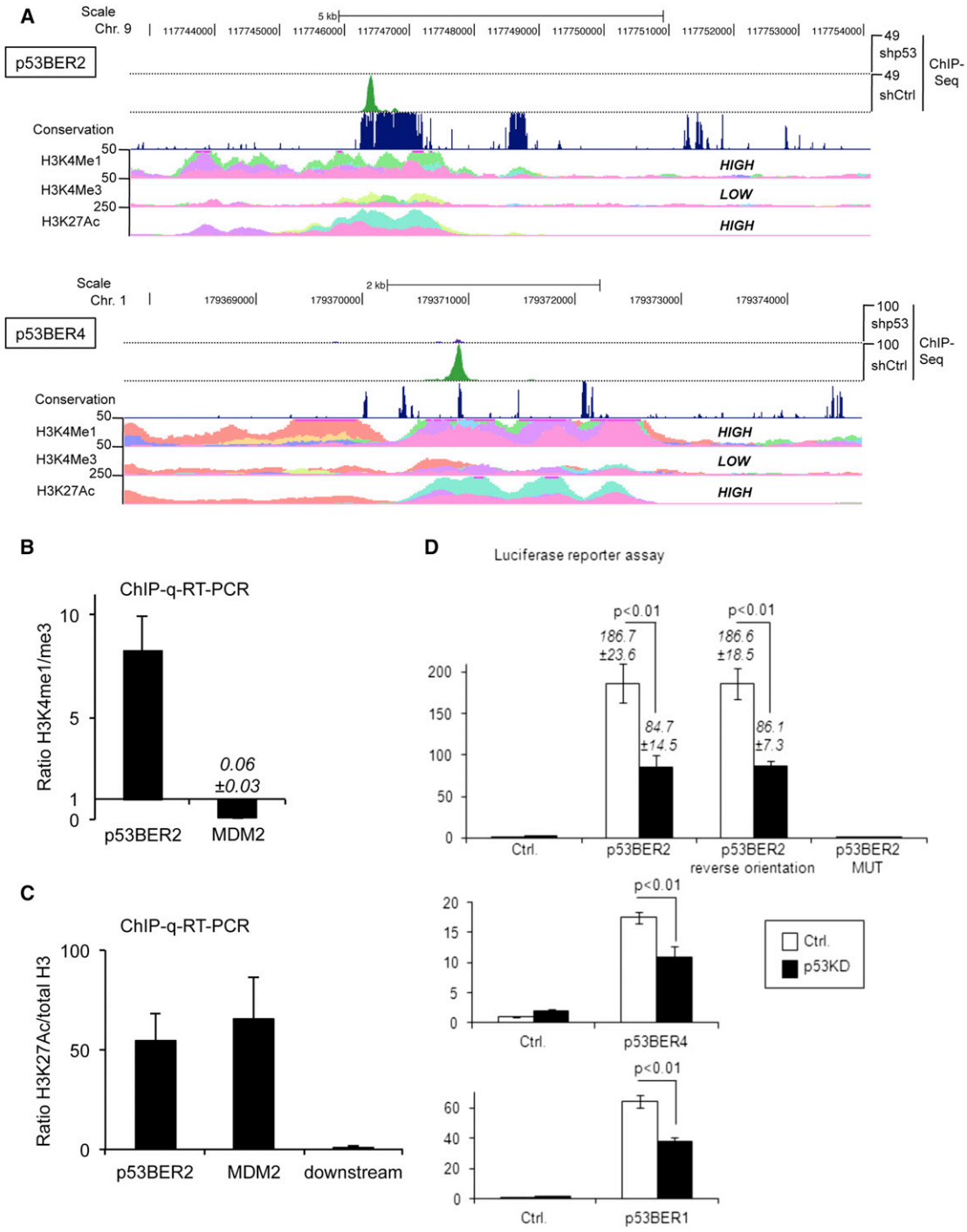

Figure 1. Identification of p53-Dependent Enhancer Domains

(A) UCSC Genome Browser (hg18 assembly) presentation of the p53-binding pattern (in BJ/ET cells expressing either a control or $p53^{KD}$ vector) (Drost et al., 2010) and histone modifications (ENCODE Project Consortium) at the p53BER2 (top) and p53BER4 (bottom) genomic regions. Different cell lines in the histone modification track are associated with a particular color.

(B) BJ/ET cells were subjected to ChIP for total H3, H3K4me1, and H3K4me3. The abundance of the histone modifications within the indicated genomic regions was calculated as the ratio between the H3K4me1 and H3K4me3, both corrected to total H3. MDM2 was used as promoter control. Graphs show means and SD for three independent experiments.

(C) Cells from (B) were subjected to ChIP with antibodies against total H3 and H3K27Ac. H3K27Ac abundance within the indicated genomic regions was calculated as the ratio between H3K27Ac and total H3. MDM2 was used as promoter control. Region downstream of p53BER2 was used as negative control. Graphs show means and SD for three independent experiments.

(legend continued on next page)

Collectively, our observations strongly suggest that the identified p53-bound enhancer regions physically contact multiple distant genomic regions to convey p53-dependent transcription regulation.

p53BER2 and p53BER4 Produce Enhancer RNAs in a p53-Dependent Manner

Recently, it was shown that RNA polymerase II (RNAPII) binds to a subset of enhancers where it bidirectionally transcribes so-called enhancer RNAs (Kim et al., 2010). eRNAs are noncoding, nonpolyadenylated RNAs with sizes of up to 2 kb. In addition to high levels of H3K4me1, low levels of H3K4me3, and high levels of H3K27Ac, eRNA-producing enhancer domains were marked by RNAPII and p300/CBP binding (Kim et al., 2010). We found association of RNAPII and p300 with p53BER2 and p53BER4 in different cell lines (ENCODE Project Consortium, 2011; Figure 3A) and confirmed this for RNAPII in BJ/ET cells by ChIP (Figure 3B). No RNAPII and p300 association was detected in control downstream regions. Furthermore, we found increased p53 binding on p53BER2 and p53BER4 after p53 activation by Nutlin-3 treatment (Figure 3C), and reporter assays with constructs in which p53BER2 was cloned upstream of a promoter-less luciferase gene revealed p53-dependent promoter activity (Figure S3A). Next, we asked whether p53 induces transcript production from p53BER2 and p53BER4. We activated p53 in BJ/ET cells with Nutlin-3 and performed quantitative RT-PCR (qRT-PCR) analysis, which revealed transcript induction at both loci upon Nutlin-3 treatment (Figure 3D). Similarly, in MCF7 cells too, transcript production could be induced from p53BER2 and p53BER4 upon ionizing radiation or Nutlin-3 treatment (Figures S3B and S3C). In contrast, no transcript was detected from these enhancer regions either in cells knocked down for p53 or in Nutlin-3-treated MDA-MB-436 cells, which contain mutant p53 (Figures S3D–S3F), further confirming p53 dependency. Northern blot analysis detected Nutlin-3-induced production of a transcript at p53BER2 with a size of about 600 nucleotides (Figure 3E). In addition, we were able to identify the 5′ start site of the p53BER2-produced transcript (Figure S3G). Last, transcripts produced from p53BER2 and p53BER4 were reproducibly detected upon p53 activation by qRT-PCR on random-primed complementary DNA (cDNA), whereas qRT-PCRs on oligo(dT)-primed cDNA failed to do so, implying that the detected transcripts are likely to be nonpolyadenylated. This is in accordance with the recent observation that eRNAs lack poly(A) tails (Kim et al., 2010). In conclusion, our observations indicate that p53BER2 and p53BER4 produce eRNAs in a p53-dependent manner.

Enhancer RNAs Are Functional Noncoding RNAs that Enhance Transcription

The production of eRNAs at enhancers has been shown to correlate with transcription of neighboring genes, but their functional involvement is unclear (Kim et al., 2010). Therefore, we set out to investigate whether eRNAs are involved in enhancement of transcription. We cloned three regions surrounding the p53 binding site in p53BER2 into a vector containing 24 copies of the MS2 hairpin RNA structure to generate a chimera RNA with the 24 copies of MS2 (Figure 4A). The MS2 hairpin binds tightly to the MS2-coat viral protein (MS2-CP) (Haim-Vilmovsky et al., 2011). We attached the Gal4 DNA-binding domain to MS2-CP and designed a luciferase reporter vector containing 5× Gal4 binding sites upstream of a promoter. If the cloned region produces RNA that is functionally involved in transcription enhancement, cotransfection of all components (eRNA-MS2, Gal4-MS2-CP, and the luciferase reporter) would localize the RNA nearby the promoter and is expected to enhance reporter activity (Figure 4A). Intriguingly, cotransfection of region 1, but not 2 or 3, significantly enhanced reporter activity (Figure 4B). We performed MS2-CP pull-down assays to verify transcript production from region 1 and to exclude plasmid contamination in the (semi-) qRT-PCR (Figure 4C). Since p53BERs contain p53-dependent promoter activity (Figure S3A), we tested whether p53 binding is required for enhancing activity in this assay. Figure 4C shows that mutation of all p53 sites in p53BER2 markedly reduced transcript levels, as determined by MS2-CP pull-down assays, supporting p53-dependent eRNA production from this region. Moreover, transfection of this reporter did not result in any transcription enhancement activity by region 1 (Figure 4D), showing that the enhancing effect is dependent on p53 binding and production of the transcript. Furthermore, removal of the MS2-CP tethering component significantly reduced the enhancing effect of region 1 on the reporter, indicating that transcript localization is involved in the observed effect (Figure 4E). The remaining MS2-CP-independent transcriptional activation can be attributed to the overexpression of the eRNA-MS2 in the nucleus.

Altogether, these results demonstrate a role for eRNAs in transcription enhancement.

eRNAs Produced from p53BERs Are Required for Transcription Enhancement of Neighboring Genes and for an Efficient p53-Dependent Cell-Cycle Arrest

As the identified p53BERs interact with and regulate transcription of neighboring genes at distant locations, we set out to investigate whether the eRNAs produced from p53BER2 and p53BER4 are involved in p53-dependent transcriptional regulation of genes encoded in their vicinity. We designed small interfering RNAs (siRNAs) to target the eRNAs that are produced from these regions. Transfection of MCF7 cells with si-p53BER2 and si-p53BER4, but not control siRNAs, reduced corresponding eRNA transcript levels after p53 activation by Nutlin-3 (Figure S4). The genes nearest to p53BER2 and p53BER4 are *PAPPA* and *IER5*, respectively. We showed in Figures 2 and S2B that the *PAPPA* and *IER5* genes are transcribed in a p53-dependent manner and that they physically interact with the nearest p53BER domains. Moreover, no p53-binding peak was detected

(D) MCF7 cells were cotransfected with the indicated reporter construct and either control or p53 knockdown (p53KD) vector. The relative firefly luciferase/renilla activity was determined and compared to the control promoter vector (Ctrl.). Graphs represent mean and SD from three independent experiments. p values were calculated with a t test. Mutant (mut) contains point mutations in the p53-binding motifs of p53BER2.
See also Figure S1 and Table S1.

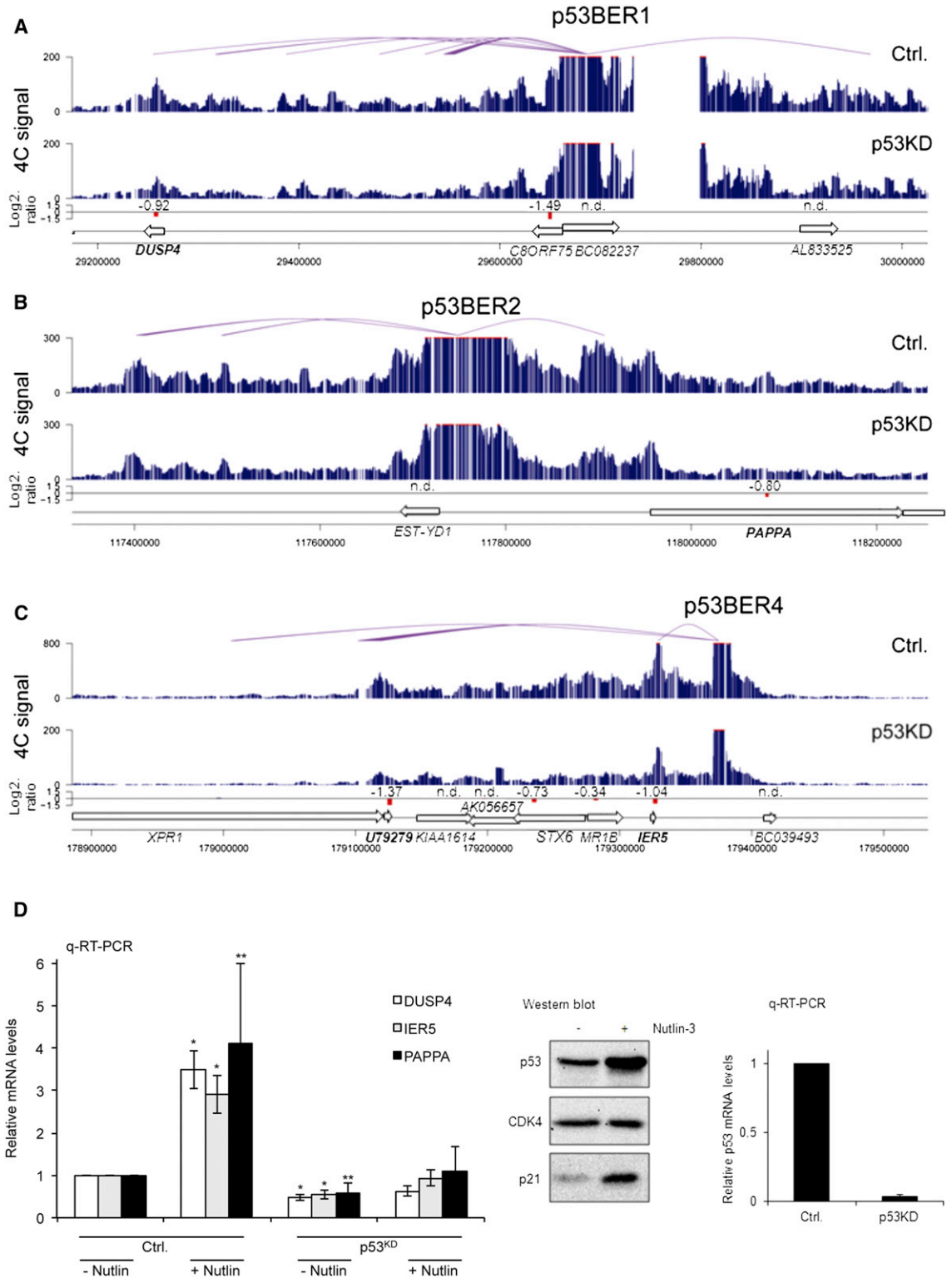

Figure 2. p53BERs Show Long-Range Interactions with Multiple Distantly Located Genes

(A–C) Long-range interactions of p53BER1, p53BER2, and p53BER4 with surrounding regions as determined by 4C in wild-type and $p53^{KD}$ BJ/ET cells. Plots represent running mean analysis in which 4C sequencing read counts were averaged over windows of 31 restriction ends. To account for the fact that the majority of the data are very close to the viewpoint, we set the data range of the vertical axis to the 98% quantile value for the analyzed region (fragments with values above the 98% quantile value are marked red on top). Arcs designate significant interactions ($p < 10^{-5}$, see also Figure S4) of the p53BERs with surrounding loci. Relative

(legend continued on next page)

in the promoters of PAPPA and IER5 by ChIP-seq in BJ/ET cells (Drost et al., 2010) that can explain such p53-dependent regulation. Therefore, we examined the effect of si-p53BER2 and si-p53BER4 on the transcription induction of PAPPA and IER5, respectively, after p53 activation. We transfected cells with a negative control siRNA, two independent siRNAs targeting p53BER transcripts, or an siRNA targeting p53 and determined the relative induction of PAPPA and IER5 mRNA levels upon Nutlin-3 treatment. As expected, transcription of PAPPA and IER5 was activated upon Nutlin-3 treatment (Figures 5A and 5B). This induction was significantly decreased when p53 was knocked down, again confirming that transcription is p53 dependent. Intriguingly, transfection of either of two independent siRNAs targeting the eRNAs produced from p53BER2 and p53BER4 significantly inhibited the induction of PAPPA and IER5, respectively, upon Nutlin-3 treatment (Figures 5A and 5B). This effect was further confirmed by RNAPII ChIP, showing that significantly less RNAPII is present at the *PAPPA* and *IER5* genes upon eRNA knockdown (Figure S5A). Thus, we conclude that eRNAs produced from p53BER2 and p53BER4 are required for the efficient induction of PAPPA and IER5 transcription, respectively, after p53 activation.

To determine whether other p53BER-interacting genes also show eRNA-dependent transcription, we investigated the levels of the p53BER4-interacting gene *U79279*. RNA-seq showed marked p53-dependent transcription of this gene (Figure 2C). Once again, transfection of siRNAs targeting p53BER4-produced eRNAs resulted in a significantly decrease in U79279 transcript induction, further supporting a role for eRNAs in enhancement of transcription (Figure S5B).

Next, we set out to investigate whether eRNA production is required for p53 function after stress induction. We transfected MCF7 cells with control siRNAs, siRNAs targeting the p53BER2 eRNA, or p53. After treatment with ionizing radiation (IR), cell-cycle profiles were analyzed by flow cytometry. As expected, while control-transfected MCF7 cells entered a G1 arrest upon IR, knockdown of either p53 or p21 did not (Figure S6A), confirming that the arrest is indeed dependent on a functional p53 pathway. Interestingly, targeting of p53BER2-produced transcripts (two distinct siRNAs) resulted in a significant decrease in the amount of cells arrested in G1 (Figures S6A and S6B). Furthermore, similar to the knockdown of p53BER2-produced eRNAs, knockdown of PAPPA also significantly inhibited induction of a p53-dependent cell-cycle arrest (Figures 5C and S6C). Neither knockdown of the p53BER2-produced transcript nor knockdown of PAPPA significantly affected p21 mRNA levels (Figure S6D). Altogether, these results indicate that the eRNAs produced from p53BER2 are required for an efficient p53-dependent cell-cycle arrest and that this effect could be mediated through inhibition of PAPPA induction by p53.

DISCUSSION

We describe here a mechanism whereby p53 induces target gene transcription through the production of eRNAs from distantly located enhancer domains. We identified several such enhancer regions (p53BERs) that are bound by p53 with high affinity, require p53 for their activity, and produce eRNAs in a p53-dependent manner. Recently, enhancer-like features were also ascribed to a different class of ncRNAs (Ørom et al., 2010). Knockdown of these ncRNAs was demonstrated to result in decreased expression of neighboring genes. In contrast to eRNAs (Kim et al., 2010), these ncRNAs are polyadenylated and the regions encoding them harbor the chromatin signature of protein-coding genes (high H3K4me3 at the 5′ end and downstream H3K36me3 [Ørom et al., 2010]). We report that the suppression of p53-induced eRNAs results in altered p53-dependent transcription of genes encoded in the vicinity of the p53BER and that eRNA expression enhances transcriptional activity in an RNA tethering reporter assay. Therefore, our results demonstrate the involvement of eRNAs in enhancement of target gene transcription, implying that they are not merely byproducts of gene transcription. This classifies eRNAs as a family of regulatory RNAs that enhance gene transcription.

In addition, we show that our identified p53BERs interact with multiple distant protein-coding genes, and we link them to the p53 network present in our cellular model system. As enhancers can interact and regulate multiple target genes (recently reviewed in Splinter et al., 2011; Ong and Corces, 2011), enhancer-bound p53 would be able to regulate transcription of multiple genes via one single genomic binding site. We propose that enhancer-bound p53 can enhance transcription of distant target genes by getting in close proximity of target gene promoters via intrachromosomal interactions. Transcription of target genes is enhanced upon p53 activation, which requires p53-dependent eRNA production (Figure 6). As the long-range interactions are not dependent on p53, the eRNAs seem to act on pre-existing chromatin conformations, which may allow for rapid induction of p53 target genes in response to diverse stimuli.

One of the genes regulated by p53BER2 is the *PAPPA* gene. PAPPA is an IGFBP protease that cleaves IGFBP4 and IGFBP5 (Lawrence et al., 1999; Conover et al., 2004), which have both shown to be involved in cell-cycle regulation and senescence (Kojima et al., 2012). Therefore, the involvement of PAPPA in cellular proliferation might be explained by its ability to regulate IGF levels. A recent publication reported p53-binding in intron 1 of the *PAPPA* gene by overexpressing p53 in the p53-negative cell line MDA-MB157 cells, which results in PAPPA repression (Chander et al., 2011). In contrast to this result, we did not detect any p53 binding within the first intron of PAPPA using p53 ChIP-seq in BJ cells and other cell lines (Figure S6E for

changes in mRNA expression upon $p53^{KD}$ were measured by 3′ end mRNA sequencing in BJ/ET cells and is represented at the bottom (red bars and numbers). n.d., not detectable. Note that significant interactions are largely unaffected in $p53^{KD}$ BJ/ET cells.

(D) BJ/ET cells expressing either a control or p53 knockdown vector were treated with Nutlin-3 for 24 hr or left untreated. Left and right panels: relative DUSP4, IER5, PAPPA, and p53 mRNA levels were measured by qRT-PCR and are represented as fold induction from values measured in untreated control cells. Graphs show means and SD for three independent experiments. p values were calculated with a t test. *$p < 0.01$, **$p < 0.05$. Middle panel: western blot analysis was performed for detection of p53 stabilization and p21 induction upon Nutlin-3 treatment. CDK4 was used as a loading control.

See also Figure S2 and Table S2.

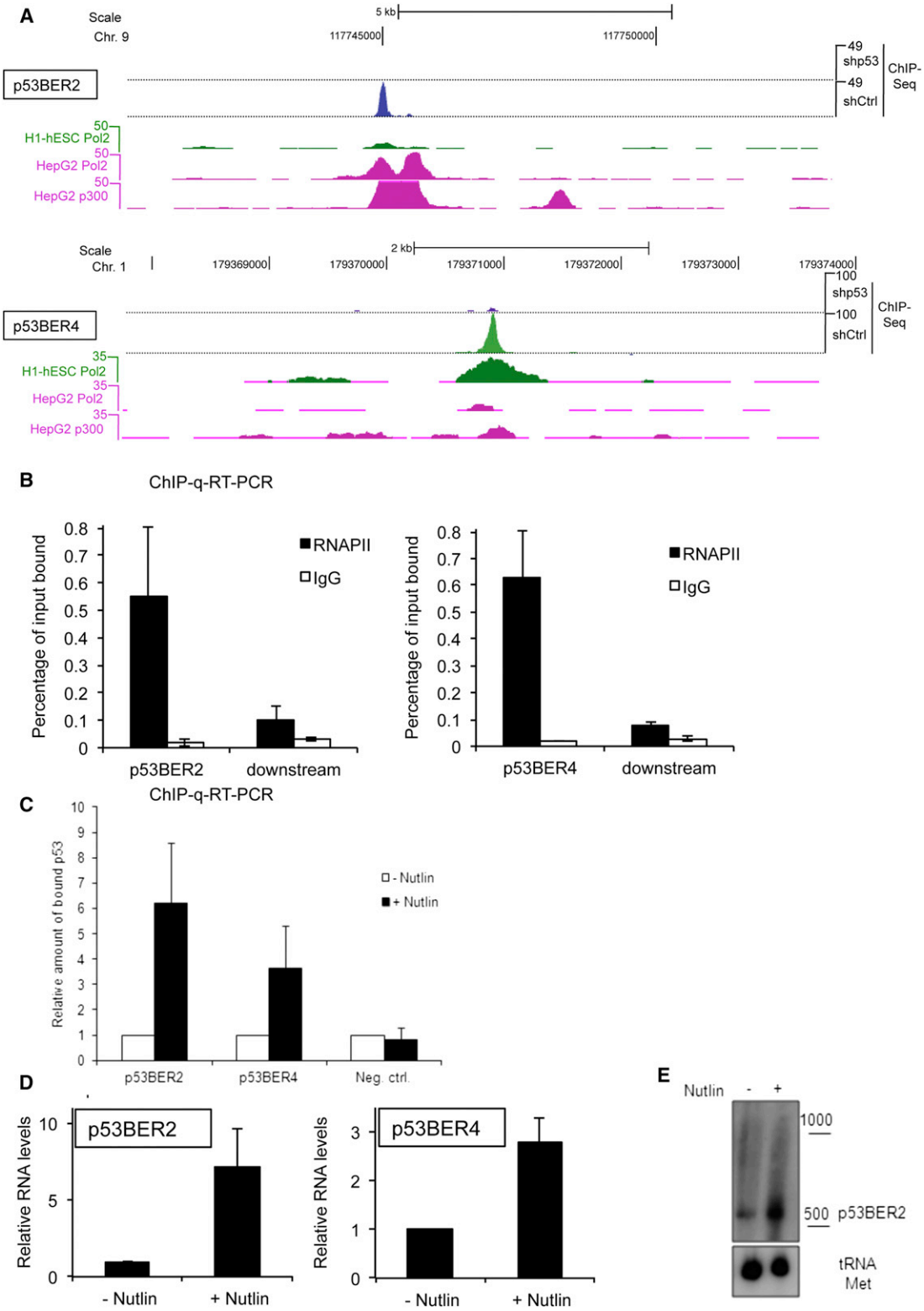

Figure 3. p53BER2 and p53BER4 Carry Features of eRNA-Producing Enhancer Domains and Produce Transcripts in a p53-Dependent Manner

(A) UCSC Genome Browser (hg18 assembly) presentation showing RNAPII and p300 binding at p53BER2 (top) and p53BER4 (bottom) (ENCODE Project Consortium).

(legend continued on next page)

BJ/ET cells). Furthermore, we report positive regulation of PAPPA transcription by p53 upon RAS^{V12} expression, Nutlin-3 treatment, and ionizing radiation (Table S2). These results imply cell type-specific regulation of PAPPA by p53. Enhancers regulate transcription in a cell type-specific manner (Ong and Corces, 2012), which could thus explain the difference in PAPPA regulation in different cell types.

Li et al. (2012) recently showed that in mouse embryonic stem cells (ESCs), p53 represses transcription of ESC-specific genes through binding and interfering with distal enhancers (Li et al., 2012). It has become clear in recent years that enhancers are marked by different histone modifications in different cell types, reflecting their cell type specificity (Ong and Corces, 2012). This means that p53 can, by binding to enhancers and regulating their activity, affect target gene transcription in a cell type-dependent manner. Further research is needed to determine what other factors determine whether p53 is required for, or interferes with, enhancer activity.

Moreover, an enhancer can interact with and regulate multiple genes. We show that eRNA knockdown interferes with transcription enhancement. Inhibition of eRNAs produced from a single enhancer could thus affect transcription of multiple genes. Therefore, eRNA inhibition could be an efficient strategy to interfere with enhancer activity. In addition, deletion of a single enhancer locus could result in the aberrant regulation of a set of genes. The genomic region including p53BER2 is located at 9q33.1. This region is associated with loss of heterozygosity in human cancer (Schultz et al., 1995; Callahan et al., 2003). Based on the data we present in this report, it would be interesting to determine whether loss of p53BERs contributes to human cancer.

EXPERIMENTAL PROCEDURES

Cell Culture, Transfection, and Retroviral Transduction

Cells were cultured in DMEM with 10% FCS and antibiotics. Transfection of MCF7 cells for reporter assays was performed with polyethylenimine. siRNA transfections of BJ/ET and MCF7 cells were performed with Dharmafect 1 and Dharmafect 3 (Dharmacon), respectively. siRNA sequences were as follows: p53BER2#1, 5′-GCACAGATTCCGTGTAAAT-3′; p53BER2#3, 5′-GCTGGACACTGGGTAAATC-3′; p53BER4#1, 5′-TTAGGGGAAGCTGCTATGT-3′; p53BER4#2, 5′-CAGCCTTGTGGTTTCACAG-3′; sip21, 5′-GACCATGTGGACCTGTCAC-3′; and sip53, 5′-GACTCCAGTGGTAATCTAC-3′. siRNAs targeting PAPPA were purchased from Dharmacon. Retroviruses were made by calcium phosphate transfection of Ecopack 2 cells (Clontech) and harvesting 40 and 64 hr later.

Constructs and Antibodies

pRetrosuper (pRS), pRS-blast, pRS-hygro, pBabe-puro-Ras^{V12}ER^{TAM}, pMSCV-blast-Ras^{V12}ER^{TAM}, and pBabe-H2B-GFP-hTERT were described previously (Voorhoeve and Agami, 2003; Brummelkamp et al., 2002b; Kolfschoten et al., 2005). pRS-p53 was previously described (Voorhoeve and Agami, 2003). So that enhancer activity could be monitored, the sequences of interest were cloned in pGL3-promoter luciferase reporter vectors (Promega). Primer sequences are shown in Table S3. Mutations in the p53-binding sequences of p53BER2 were made in two steps with the Quickchange Site-Directed mutagenesis kit (Agilent) according to manufacturer's instructions (primer 1, 5′-CTTCTGAGAAACTCATGGAGATTTCTGTGCATGCCTGAAC-3′; primer 2, 5′-ATGTCTGTGCATGCCTGAAATTCTCTGACAAAGCCAAGCA-3′).

For ChIP, antibodies against the following proteins were used: H3 (Cell Signaling Technology), H3K4me1 (Abcam, ab8895), H3K4me3 (Upstate, clone MC315), H3K27Ac (Abcam, ab4729), and RNAPII (Upstate, clone CTD4H8).

For western blotting, antibodies against p53 (DO1), p21 (F5), and CDK4 (C22) were purchased from Santa Cruz Biotechnology. Anti-beta-actin antibody was from Abcam (ab8227).

Encode Consortium Histone Modification and Protein Binding Data

For histone modifications, we used the ENCODE Promoter-Associated Histone Mark data set (H3K4me1, H3K4me3, and H3K27Ac) on nine cell lines (Gm12878, H1 ES, HepG2, HMEC, HSMM, HUVEC, K562, NHEK, and NHLF). For RNAPII and p300, we used the Histone Modifications by ChIP-seq from ENCODE/Broad Institute data set from HepG2 and H1 ESCs. Presence of histone modifications and protein binding were verified by ChIP qRT-PCR in BJ/ET cells.

Quantitative RT-PCR, 3′ End mRNA Sequencing, and Northern Blot

Total RNA was extracted with Trizol (Life Technologies) according to the manufacturer's instructions. cDNA was transcribed with Superscript III (Life Technologies) with random hexamers (for eRNAs) or oligo(dT) (for mRNAs) in accordance with the manufacturer's protocol. For determination of RNA expression levels, primers were designed with Primer Express v. 3.0 Software. Real-time PCR was performed with SYBR Green PCR master mix (Applied Biosystems) and the Chromo4 Real-Time PCR Detector (Bio-Rad Laboratories). Primer sequences are shown in Table S4.

3′ mRNA sequencing was performed according to the manufacturer's instructions (Illumina mRNA-seq). For sequencing from the 3′ end, first-strand cDNA synthesis was performed with oligo(dT) instead of random primers.

For northern blot, 30 μg total RNA (DNase treated) was run on a gel composed of 15% polyacrylamide (19:1), 48% urea, and 1× TBE. RNA was transferred to BrightStar-Plus Positively Charged Nylon Membranes (Ambion) at 200 mA for 1 hr in 0.5× TBE. Subsequently, RNA was crosslinked to the membrane (1,200 J for 1 min). Prehybridization was performed in ULTRAhyb-Oligo solution (Ambion) for 1 hr at 42°C. Hybridization was performed in ULTRAhyb-Oligo solution (Ambion) containing 150 ng biotin-tagged oligo (BioTeg; Sigma) by overnight incubation at 42°C. Next, membranes were washed in 2× SSPE/0.5% SDS (2× 15 min), 0.2× SSPE/0.5% SDS (2× 30 min), and 2× SSPE (1× 5 min). Signal detection was performed with the BrightStar BioDetect Kit according to the manufacturer's instructions (Ambion). The p53BER2 probe sequence was 5′-CCCCACTTTCCACTGGGTCC-3′.

p53BER2 5′ End Identification

Total RNA from Nutlin-3-treated BJ/ET cells was extracted with Trizol (Life Technologies) according to the manufacturer's instructions. Total RNA was used for first-strand cDNA synthesis (SuperScript III reverse transcriptase;

(B) BJ/ET cells were cultured in the presence of Nutlin-3 for 24 hr and subsequently subjected to ChIP for RNAPII. Rabbit IgG was used as negative control. Protein binding to the indicated genomic regions was quantified by calculating the percentage of input that is chromatin bound. Graphs show means and SD for three independent experiments.

(C) BJ/ET cells were cultured in the absence or presence of Nutlin-3 for 24 hr and subsequently subjected to ChIP for p53. Protein binding to the indicated genomic regions was quantified by caclucation of the percentage of input that is chromatin bound and is represented as fold induction from values measured in untreated cells. A non-p53-bound region was used as negative control. Graphs show means and SD for three independent experiments.

(D) BJ/ET cells were treated with Nutlin-3 for 24 hr or left untreated. The relative transcript levels produced at p53BER2 and p53BER4 were determined by q-RT-PCR in relation to GAPDH. Graphs show mean and SD for three independent experiments.

(E) MCF7 cells were treated with Nutlin-3 for 24 hr or left untreated. Northern blot analysis was performed to detect transcripts produced at p53BER2. tRNA-Met was used as a loading control.

See also Figure S3.

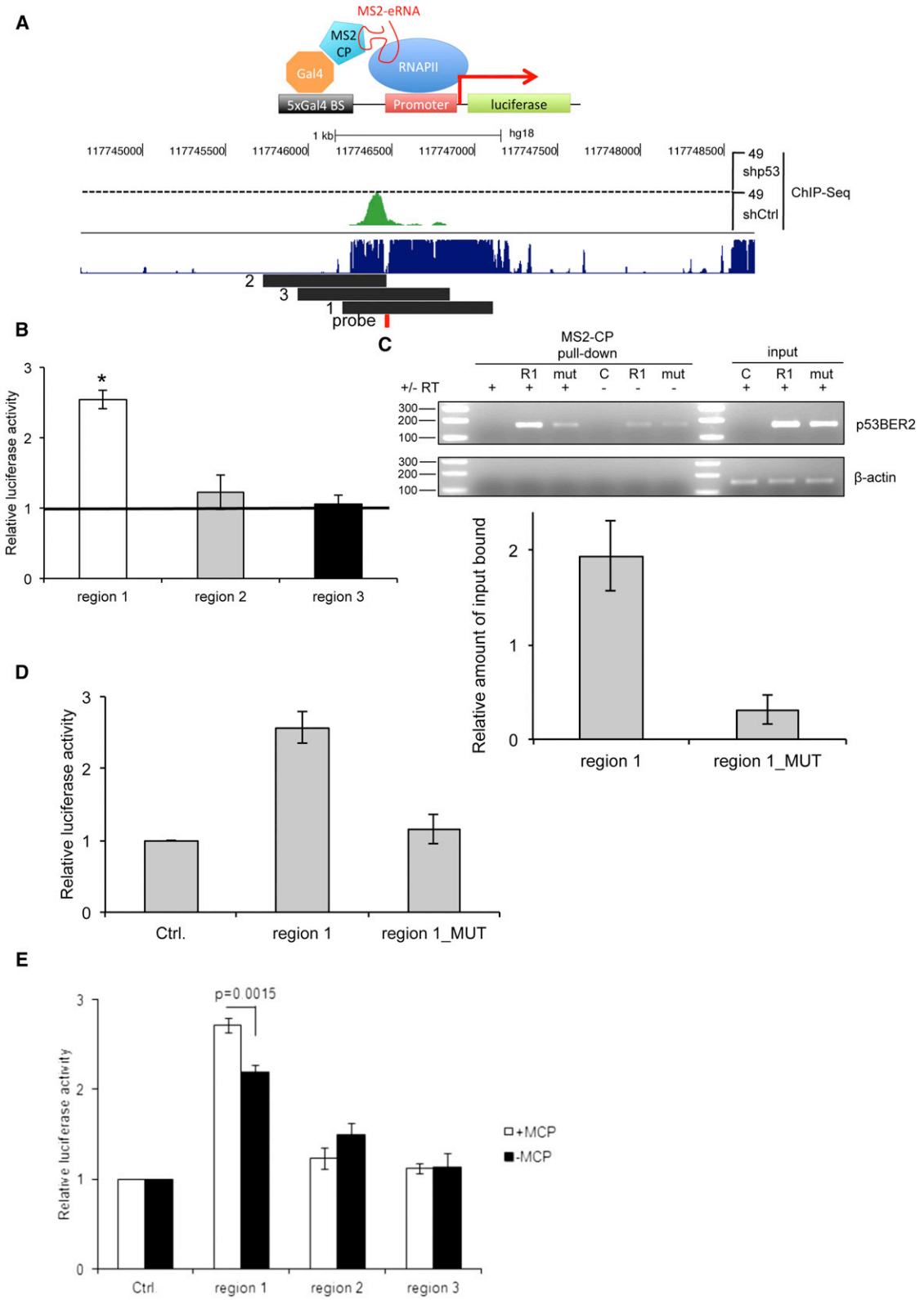

Figure 4. eRNAs Are Involved in Enhancement of Transcription

(A) Top: schematic representation of the tethering system. Bottom: location of the tested regions and the northern probe (red bar) that was used in Figure 3D.

(legend continued on next page)

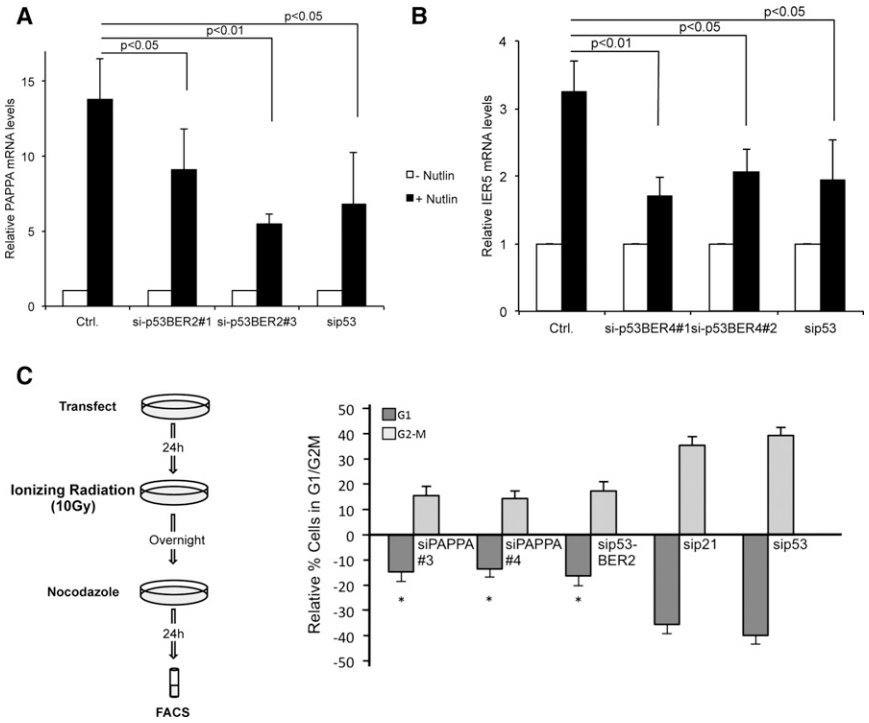

Figure 5. p53-Dependent eRNAs Are Required for Transcription of Genes Surrounding p53BER2 and p53BER4

(A and B) BJ/ET (A) and MCF7 (B) cells were transfected with the indicated siRNAs and either treated with Nutlin-3 for 24 hr or left untreated. Relative PAPPA (A) and IER5 (B) mRNA levels were measured by qRT-PCR and are represented as the fold induction from values measured in untreated cells. Graphs represent mean and SD from at least three independent experiments. p values were calculated with a t test.

(C) On the left is a schematic representation of the time line used for cell-cycle analysis. At the right side are the cell-cycle distribution changes of MCF7 cells transfected with control siRNA or siRNAs against p53BER2 (sip53BER2) and PAPPA (siPAPPA#3 and siPAPPA#4) treated with ionizing radiation (10 Gy). For capture of cycling cells in G2/M, cells were incubated 24 hr with nocodazole before flow cytometric analysis. For each condition, the difference between the control transfected and indicated siRNAs was calculated and plotted as the relative variation of cells present in both G1 and G2/M phase. Graphs represent mean and SD from three independent experiments. p values were calculated with a t test. *$p < 0.01$. See also Figures S4–S6.

Life Technologies) with a p53BER2-specific RT primer (5′- CCCCACTTTC CACTGGGTCC-3′). Single-strand cDNA was converted to double-strand cDNA (Life Technologies) and end repaired for 30 min at 20°C (NEBNext End Repair Enzym Module [New England Biolabs] supplemented with 1 μl Klenow DNA polymerase [Life Technologies]). After purification (QIAquick PCR Purification Kit; QIAGEN), 1 μl 45 μM annealed P5-splinkerette (5′-AAT GATACGGCGACCACCGAGATCTACACTCTTTCCCTACACGACGCTCTTCC GATCT-3′) was ligated overnight at 16°C to the cDNA. The P5-splinkerette-ligated cDNA was purified (QIAquick PCR Purification Kit; QIAGEN) and used as template for PCR with P5 primer (5′-AATGATACGGCGACCACCGA GATCT-3′) and p53BER2-specific nested primers (nested_1, 5′-CCCAGTG GAAAGTGGGGGAG-3′; nested_2, 5′- GTGGAAAGTGGGGGAGTGGTG-3′) with Phusion Hot Start DNA polymerase (Finnzymes). After gel purification (QIAgen Gel Extraction Kit; QIAGEN), the DNA was cloned into pCR-Blunt (Zero Blunt PCR Cloning kit; Life Technologies) and transformed into competent bacteria. Plasmid DNA was purified and sequenced.

Luciferase Reporter Assays

MCF7 cells were cotransfected with 400 ng pRS or pRS-p53^{KD} in combination with 100 ng luciferase reporter (pGL3-promoter; Promega) and 5 ng renilla plasmid. Three days after transfection, luciferase assays were performed in accordance with the manufacturer's instructions (Dual Luciferase system; Promega). For RNA tethering, MCF7 cells were cotransfected with chimeras of different regions around p53BER2 and 24 copies of MS2 in pSUPER (Brummelkamp et al., 2002a), pCS2-empty, or pCS2-MCP:GAL4, and pGL3 containing five copies of the GAL4 binding site in front of the SV40 promoter. Three days after transfection, luciferase assays were performed in accordance with the manufacturer's instructions (Dual Luciferase system; Promega).

Chromatin Immunoprecipitation Assay

ChIP assays were performed as described (Dahl and Collas, 2008) with some minor modifications. In brief, cells were crosslinked for 8 min with 1% formaldehyde and neutralized with 125 mM glycine. After centrifugation, the pellet was resuspended in lysis buffer (50 mM Tris [pH 8.0], 10 mM EDTA, and 1% SDS) and sonicated to achieve an average fragment size of 300–800 bp. Chromatin was diluted in RIPA buffer (10 mM Tris [pH 7.5], 140 mM NaCl, 1 mM EDTA, 0.5 mM EGTA, 1% Triton X-100, 0.1% SDS, and 0.1% sodium deoxycholate) and incubated overnight with the indicated antibody. A negative control for immunoprecipitation was performed in the presence of normal rabbit IgG (Santa Cruz). The next day, beads were added and incubated for 2–3 hr. After washing, DNA was eluted overnight in elution buffer (20 mM Tris [pH 7.5], 5 mM EDTA, 50 mM NaCl, 1% SDS, and 50 μg/ml proteinase K) followed by DNA purification with a PCR purification kit (Roche). Real-time PCR was performed with SYBR Green PCR master mix (Applied Biosystems) and the Chromo4 Real-Time PCR Detector (Bio-Rad Laboratories). Primer sequences are shown in Table S5.

(B) MCF7 cells were cotransfected with a pSuper-24MS2 vector containing the indicated p53BER2 regions, and the MS2-CP:Gal4 and reporter constructs (as described in A). The relative firefly luciferase/renilla activity was determined compared to the control promoter vector (set to 1). Graphs represent mean and SD from three independent experiments. p values were calculated with a t test. *$p < 0.01$.

(C) MCF7 cells were transfected with empty pSuper-24MS2 vector (C), pSuper-region 1-24MS2 (R1), or pSuper-region 1_MUT-24MS2. MS2-CP pull-down assays followed by RT-PCR with p53BER2 primers were performed to verify transcript production. Expected PCR product size 166 bp. Bottom graph: transcript levels produced from region 1 and region 1_MUT were determined with MS2-CP pull-down assays followed by RT-PCR. Graphs show means and SD for three independent experiments.

(D) MCF7 cells were cotransfected as in (B) with either wild-type region 1 or region 1 containing point mutations in the p53-binding motifs (MUT). The relative firefly luciferase/renilla activity was determined and compared to the control promoter vector (Ctrl.). Graphs represent mean and SD from three independent experiments.

(E) MCF7 cells were cotransfected with the indicated p53BER2 regions, the reporter construct, and either MS2-CP:Gal4 or empty vector. Error bars represent the SEM (n = 7). p values were calculated with a t test.

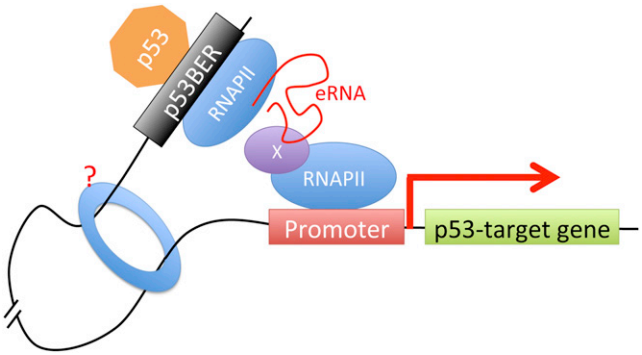

Figure 6. Schematic Model Depicting How p53BERs May Enhance Target Gene Transcription

p53-independent intrachromosomal interactions bring p53-bound p53BERs in close proximity of target genes, through yet unidentified protein complex (marked by ?). It seems likely that p53 is bound at p53BERs in a poised state and that upon p53 activation eRNAs are produced and transcription enhancement takes place. eRNAs are produced in a p53-dependent manner and affect transcription enhancement by a currently unknown mechanism. It is possible that eRNAs interact with proteins (X) that activate transcription.

MS2-CP Pull-Down Assay

MS2-CP pull-down assays were performed as described (Slobodin and Gerst, 2011). In brief, MCF7 cells were transfected with pSUPER containing region 1 or region 1_MUT (p53 binding site mutant) attached 24 copies of MS2. After 72 hr, cells were crosslinked for 10 min with 0.01% formaldehyde and neutralized with 125 mM glycine. Cells were snap frozen in liquid nitrogen and thawed in lysis buffer (50 mM Tris [pH 7.5], 150 mM NaCl, 1% Triton X-100, 1.8 mM MgCl2, and protease inhibitor cocktail [Roche]) with occasional vortexing and were subsequently sonicated. After centrifugation, supernatant was blocked with avidin solution (Sigma; 10 μg per 1 mg protein extract). Streptavidin-conjugated beads (GE Healthcare) were precoupled to MS2-CP-SBP protein and blocked in lysis buffer containing 2% BSA and yeast transfer RNA (tRNA; 0.1 mg per 100 μl beads). The blocked beads were added to the blocked protein extract and incubated overnight. After the pull-down, beads were washed twice with lysis buffer, twice with washing buffer (20 mM Tris [pH 7.5], 300 mM Nacl, and 0.5% NP40) and twice with PBS. Beads were eluted with biotin elution solution (6 mM biotin [Sigma] in PBS), and an equal volume of reverse crosslink buffer was added (100 mM Tris [pH 7.0], 10 mM EDTA, 20 mM DTT, and 2% SDS). Reverse crosslinking was performed at 70°C for 2 hr. RNA was extracted from eluted and input fractions with Trizol (Life Technologies) according to the manufacturer's instructions. cDNA was transcribed with Superscript III (Life Technologies) with random hexamers in accordance with the manufacturer's protocol. RT-PCR was performed with p53BER2-specific primers (FW, 5′-CAGTCTACATT CCCTGGCCTTTG-3′; RV, 5′-GACATGAGCCATTTTACCCTTAATCC'-3′).

Chromosome Conformation Capture on Chip

4C templates were prepared as described previously (Splinter et al., 2011). In brief, at least 10^7 BJ/ET cells (with or without p53 knockdown) were harvested with trypsin-EDTA, and trypsin was quenched with FCS-containing medium. Cells were crosslinked with 2% formaldehyde for 10 min at room temperature, followed by quenching with glycine (125 mM final) and centrifugation for 8 min at 600 g (4°C). Cells were lysed in 150 mM NaCl, 50 mM Tris-HCl (pH 7.5), 5 mM EDTA, 0.5% NP-40, and 1.0% Triton X-100, and nuclei were pelleted for 8 min at 600 × g (4°C). Nuclei were digested overnight with 400 U DpnII (NEB) or Csp6I (Fermentas), followed by proximity ligation in 7 ml with 100 U T4 DNA ligase (Roche) overnight at 16°C. DNA circles were phenol-chloroform extracted and ethanol precipitated with glycogen as a carrier (20 μg/ml). DNA circles were further digested with 50 U Csp6I (for DpnII circles) or DpnII (for Csp6I circles) overnight at 37°C followed by heat inactivation and were subsequently ligated in 14 ml with 200 U T4 DNA ligase. Trimmed circles, the 4C template, were ethanol precipitated with glycogen as a carrier (20 μg/ml). Sixteen identical 50 μl PCR reactions were performed per viewpoint with the Expand Long Template PCR system (Roche) with 200 ng 4C template per PCR reaction. PCR conditions were as follows: 95°C for 2 min and 36 cycles of 95°C for 15 s, 55°C for 1 min, and 68°C for 3 min, followed by a final step of 68°C for 7 min. All 16 PCR reactions were pooled and purified for next-generation sequencing with the Roche High Pure PCR Product Purification Kit. Each DpnII experiment was validated in a biological replicate experiment with Csp6I, and vice versa.

4C primers carried additional 5′ overhangs composed of adaptor sequences for Illumina single-read sequencing and were sequenced on a GA-II or Hi-seq 2000 machine (Illumina). Mapping of 4C data was performed essentially as in Splinter and de Laat (2011). For visualization and identification of regions with significant enrichment of 4C signal, we generate local 4C domainograms. For generation of these graphs, genomic windows of a given size are compared to their directly flanking genomic windows via a Wilcoxon rank-sum test. Formally, the window $W_{i..i+w-1}$ is compared to the up- and downstream windows $W_{i-w..i-1}$ and $W_{i+w..i+2w-1}$, respectively, where W is a genomic window, i is the index of a fragment in the genome, and w is the size of the window. For calculation of the enrichment along the region of interest, a sliding-window approach is employed. By performance of a statistical test over a range of window sizes (w) and plotting of the resulting matrix of p values along the chromosome, a multiscale representation of the 4C data is obtained. Windows that have a p value $< 10^{-5}$ in the Wilcoxon rank-sum test are represented by arcs in Figures 2A–2C.

SUPPLEMENTAL INFORMATION

Supplemental Information includes six figures and five tables and can be found with this article online at http://dx.doi.org/10.1016/j.molcel.2012.11.021.

ACKNOWLEDGMENTS

We thank Boris Slobodin and Koos Rooijers for technical assistance and the Encode project for providing the publicly available data sets. Further, this work was supported by funds from the European Research Council (ERC), Dutch Cancer Foundation (KWF), Horizon, and Nederlandse Organisatie voor Wetenschappelijk Onderzoek (VICI-NWO) to R.A. and the Fundação para a Ciência e a Tecnologia, Portugal to C.A.M.

Received: July 6, 2012
Revised: October 16, 2012
Accepted: November 20, 2012
Published: December 27, 2012

REFERENCES

Birney, E., Stamatoyannopoulos, J.A., Dutta, A., Guigó, R., Gingeras, T.R., Margulies, E.H., Weng, Z., Snyder, M., Dermitzakis, E.T., Thurman, R.E., et al.; ENCODE Project Consortium; NISC Comparative Sequencing Program; Baylor College of Medicine Human Genome Sequencing Center; Washington University Genome Sequencing Center; Broad Institute; Children's Hospital Oakland Research Institute. (2007). Identification and analysis of functional elements in 1% of the human genome by the ENCODE pilot project. Nature *447*, 799–816.

Brady, C.A., Jiang, D., Mello, S.S., Johnson, T.M., Jarvis, L.A., Kozak, M.M., Kenzelmann Broz, D., Basak, S., Park, E.J., McLaughlin, M.E., et al. (2011). Distinct p53 transcriptional programs dictate acute DNA-damage responses and tumor suppression. Cell *145*, 571–583.

Brummelkamp, T.R., Bernards, R., and Agami, R. (2002a). A system for stable expression of short interfering RNAs in mammalian cells. Science *296*, 550–553.

Brummelkamp, T.R., Bernards, R., and Agami, R. (2002b). Stable suppression of tumorigenicity by virus-mediated RNA interference. Cancer Cell *2*, 243–247.

Callahan, G., Denison, S.R., Phillips, L.A., Shridhar, V., and Smith, D.I. (2003). Characterization of the common fragile site FRA9E and its potential role in ovarian cancer. Oncogene *22*, 590–601.

Chander, H., Halpern, M., Resnick-Silverman, L., Manfredi, J.J., and Germain, D. (2011). Skp2B overexpression alters a prohibitin-p53 axis and the transcription of PAPP-A, the protease of insulin-like growth factor binding protein 4. PLoS ONE *6*, e22456.

Christophorou, M.A., Ringshausen, I., Finch, A.J., Swigart, L.B., and Evan, G.I. (2006). The pathological response to DNA damage does not contribute to p53-mediated tumour suppression. Nature *443*, 214–217.

Conover, C.A., Bale, L.K., Overgaard, M.T., Johnstone, E.W., Laursen, U.H., Füchtbauer, E.M., Oxvig, C., and van Deursen, J. (2004). Metalloproteinase pregnancy-associated plasma protein A is a critical growth regulatory factor during fetal development. Development *131*, 1187–1194.

Creyghton, M.P., Cheng, A.W., Welstead, G.G., Kooistra, T., Carey, B.W., Steine, E.J., Hanna, J., Lodato, M.A., Frampton, G.M., Sharp, P.A., et al. (2010). Histone H3K27ac separates active from poised enhancers and predicts developmental state. Proc. Natl. Acad. Sci. USA *107*, 21931–21936.

Dahl, J.A., and Collas, P. (2008). A rapid micro chromatin immunoprecipitation assay (microChIP). Nat. Protoc. *3*, 1032–1045.

De Santa, F., Barozzi, I., Mietton, F., Ghisletti, S., Polletti, S., Tusi, B.K., Muller, H., Ragoussis, J., Wei, C.L., and Natoli, G. (2010). A large fraction of extragenic RNA pol II transcription sites overlap enhancers. PLoS Biol. *8*, e1000384.

Dekker, J., Rippe, K., Dekker, M., and Kleckner, N. (2002). Capturing chromosome conformation. Science *295*, 1306–1311.

Drost, J., Mantovani, F., Tocco, F., Elkon, R., Comel, A., Holstege, H., Kerkhoven, R., Jonkers, J., Voorhoeve, P.M., Agami, R., and Del Sal, G. (2010). BRD7 is a candidate tumour suppressor gene required for p53 function. Nat. Cell Biol. *12*, 380–389.

ENCODE Project Consortium. (2011). A user's guide to the encyclopedia of DNA elements (ENCODE). PLoS Biol. *9*, e1001046.

Guttman, M., Amit, I., Garber, M., French, C., Lin, M.F., Feldser, D., Huarte, M., Zuk, O., Carey, B.W., Cassady, J.P., et al. (2009). Chromatin signature reveals over a thousand highly conserved large non-coding RNAs in mammals. Nature *458*, 223–227.

Haim-Vilmovsky, L., Gadir, N., Herbst, R.H., and Gerst, J.E. (2011). A genomic integration method for the simultaneous visualization of endogenous mRNAs and their translation products in living yeast. RNA *17*, 2249–2255.

Heintzman, N.D., Stuart, R.K., Hon, G., Fu, Y., Ching, C.W., Hawkins, R.D., Barrera, L.O., Van Calcar, S., Qu, C., Ching, K.A., et al. (2007). Distinct and predictive chromatin signatures of transcriptional promoters and enhancers in the human genome. Nat. Genet. *39*, 311–318.

Heintzman, N.D., Hon, G.C., Hawkins, R.D., Kheradpour, P., Stark, A., Harp, L.F., Ye, Z., Lee, L.K., Stuart, R.K., Ching, C.W., et al. (2009). Histone modifications at human enhancers reflect global cell-type-specific gene expression. Nature *459*, 108–112.

Huarte, M., Guttman, M., Feldser, D., Garber, M., Koziol, M.J., Kenzelmann-Broz, D., Khalil, A.M., Zuk, O., Amit, I., Rabani, M., et al. (2010). A large intergenic noncoding RNA induced by p53 mediates global gene repression in the p53 response. Cell *142*, 409–419.

Kim, T.K., Hemberg, M., Gray, J.M., Costa, A.M., Bear, D.M., Wu, J., Harmin, D.A., Laptewicz, M., Barbara-Haley, K., Kuersten, S., et al. (2010). Widespread transcription at neuronal activity-regulated enhancers. Nature *465*, 182–187.

Kojima, H., Kunimoto, H., Inoue, T., and Nakajima, K. (2012). The STAT3-IGFBP5 axis is critical for IL-6/gp130-induced premature senescence in human fibroblasts. Cell Cycle *11*, 730–739.

Kolfschoten, I.G., van Leeuwen, B., Berns, K., Mullenders, J., Beijersbergen, R.L., Bernards, R., Voorhoeve, P.M., and Agami, R. (2005). A genetic screen identifies PITX1 as a suppressor of RAS activity and tumorigenicity. Cell *121*, 849–858.

Lawrence, J.B., Oxvig, C., Overgaard, M.T., Sottrup-Jensen, L., Gleich, G.J., Hays, L.G., Yates, J.R., 3rd, and Conover, C.A. (1999). The insulin-like growth factor (IGF)-dependent IGF binding protein-4 protease secreted by human fibroblasts is pregnancy-associated plasma protein-A. Proc. Natl. Acad. Sci. USA *96*, 3149–3153.

Li, M., He, Y., Dubois, W., Wu, X., Shi, J., and Huang, J. (2012). Distinct regulatory mechanisms and functions for p53-activated and p53-repressed DNA damage response genes in embryonic stem cells. Mol. Cell *46*, 30–42.

Ong, C.T., and Corces, V.G. (2011). Enhancer function: new insights into the regulation of tissue-specific gene expression. Nat. Rev. Genet. *12*, 283–293.

Ong, C.T., and Corces, V.G. (2012). Enhancers: emerging roles in cell fate specification. EMBO Rep. *13*, 423–430.

Ørom, U.A., Derrien, T., Beringer, M., Gumireddy, K., Gardini, A., Bussotti, G., Lai, F., Zytnicki, M., Notredame, C., Huang, Q., et al. (2010). Long noncoding RNAs with enhancer-like function in human cells. Cell *143*, 46–58.

Schultz, D.C., Vanderveer, L., Buetow, K.H., Boente, M.P., Ozols, R.F., Hamilton, T.C., and Godwin, A.K. (1995). Characterization of chromosome 9 in human ovarian neoplasia identifies frequent genetic imbalance on 9q and rare alterations involving 9p, including CDKN2. Cancer Res. *55*, 2150–2157.

Slobodin, B., and Gerst, J.E. (2011). RaPID: an aptamer-based mRNA affinity purification technique for the identification of RNA and protein factors present in ribonucleoprotein complexes. Methods Mol. Biol. *714*, 387–406.

Splinter, E., and de Laat, W. (2011). The complex transcription regulatory landscape of our genome: control in three dimensions. EMBO J. *30*, 4345–4355.

Splinter, E., de Wit, E., Nora, E.P., Klous, P., van de Werken, H.J., Zhu, Y., Kaaij, L.J., van Ijcken, W., Gribnau, J., Heard, E., and de Laat, W. (2011). The inactive X chromosome adopts a unique three-dimensional conformation that is dependent on Xist RNA. Genes Dev. *25*, 1371–1383.

Voorhoeve, P.M., and Agami, R. (2003). The tumor-suppressive functions of the human INK4A locus. Cancer Cell *4*, 311–319.

Vousden, K.H., and Lu, X. (2002). Live or let die: the cell's response to p53. Nat. Rev. Cancer *2*, 594–604.

Wang, D., Garcia-Bassets, I., Benner, C., Li, W., Su, X., Zhou, Y., Qiu, J., Liu, W., Kaikkonen, M.U., Ohgi, K.A., et al. (2011). Reprogramming transcription by distinct classes of enhancers functionally defined by eRNA. Nature *474*, 390–394.

Wei, C.L., Wu, Q., Vega, V.B., Chiu, K.P., Ng, P., Zhang, T., Shahab, A., Yong, H.C., Fu, Y., Weng, Z., et al. (2006). A global map of p53 transcription-factor binding sites in the human genome. Cell *124*, 207–219.